

SIMULATION OF CORRODED PIPES SUBJECTED TO INTERNAL EXPLOSION CONSIDERING FLUID STRUCTURE INTERACTION

Hsu Yang Shang, hsu.shang@pucpr.br

Roberto Dalledone Machado, roberto.machado@pucpr.br

Pontifícia Universidade Católica do Paraná, Programa de Pós-Graduação em Engenharia Mecânica, Rua Imaculada Conceição, 1155, CEP – 80.215-901, Curitiba, PR

Abstract. *Accidents caused by explosions should be considered in some engineering projects, such as pipeline for transportation of oil and gas. Some empirical methods are found in the literature and computational models based on finite element method are beginning to be found. This work deals with the computational modeling and simulation of corroded pipes subjected to internal explosion. The explosion suddenly unleashed a wave of pressure and temperature. A fluid structure analysis is made considering the nonlinear behavior of the material. Two defects of different depths are analyzed using the commercial software Autodyn. A Lagrangian-Eulerian formulae is used to model respectively the duct and the fluid medium. The results show different behavior between the defects and the influence of shock wave on the pipeline.*

Keywords: *Explosion, Shockwave, Fluid – Structure Interaction, Corroded Pipes*

1. INTRODUCTION

Steel pipes are the main means of transportation to natural gas and petroleum, or other chemical products. In many cases, the natural gas or chemical product are explosive substances. Once the ignition is provided, it will initiate a process of explosion, producing flame and blast wave. The blast phenomenon can be interpreted as the propagation of thermal wave and pressure wave. The explosion is characterized as a sudden increase of pressure and temperature nearby the detonation point. From this point, the pressure wave and temperature wave propagate in approximated circular form and impact any obstacle in the front. Therefore, this type of physical phenomenon can be characterized as an interaction of solid and fluid. The explosion produces a wave of high pressure and temperature, which spreads quickly in the medium fluid, producing mechanical reactions, such as stresses and deformations. In the case of inner explosion of a tube, after the explosive is detonated, the wave of pressure and temperature propagate toward to the tube wall, and obviously, there is interaction of solid – fluid.

Corrosion is a common phenomenon which occurs in industry and produce material degradation on the surface of tube, reducing its thickness and, consequently, the strength and limit pressure of transportation. An inner explosion of a tube represents a risk issue and an important area of research.

Chang and Kong (1995) have studied a model of thermal explosion considering the reaction ratio following the law of Arrhenius in a range of temperature. The authors of this work had used partial differential equation to simulate a thermal explosion with different explosives, with its respective temperature of initiation in the process. As the deduced partial differential equation does not have exact solution, therefore, the authors had considered a numerical approach solution. However, the results gathered by the authors had not been compared with any reference in literature.

Ritsu Dobashi (1997) analyzed an explosion by gas quantitatively in a closed environment, considering behavior of the turbulent gas and that generates instability in the front of the flame. This behavior also increases speed of propagation of the flame that in turn, increases the pressure of the explosion. Another factor is the distribution of concentration of the fuel that also contributes to increase the chamber pressure. The disturbance in the front of the flame can be caused by the following factors: turbulent flow of the gas, distribution not uniform of the gas concentration (air and methane) and the instability of the front of induced flame for the interaction between pressure wave and wave of flame. The numerical results gathered by the deduced equations have been compared with the experimental study carried out by the same author previously.

Kwon and Cunningham (1997) had studied the behavior of strengthened structures submitted to an underwater explosion. This explosion produces a dynamic load that reaches the structure represented by the element pipe rind. The authors had used finite elements to analyze the structure, while the water, the medium of the shock wave propagation, was meshed by boundary elements. To determine the underwater shock waves, the “doubly asymptotic approximation” method was used. And the commercial software DYNA3D was used for solution of the interaction solid-fluid.

Zyskowski et. al. (2004) had developed a study to evaluate mechanical effect of a structure submitted to an accidental explosion of mixture of gas, hydrogen with air. The main objective is to analyze and to compare different dynamic methods analysis. In this study, the authors had searched a suitable strategy to analyze a structure submitted to the internal wave of shock. It was carried out a experimental study and a numerical study. Such numerical analysis has adopted two steps. The first one is the evaluation of pressure produced by a detonation of TNT in an experiment, adopting the law of scale of Hopkinson, and after that, introduces the pressure into Autodyn software. And also, a simplified method considered by Baker was verified (analytical model). In this study, the authors considered the walls

of the structure, or obstacle ahead the shock wave, as being infinitely rigid. Such consideration is a merely simplification. However it is a conservative approach. The authors of this work, had only validated Autodyn software result, and verified if this software is capable to capture the reflected wave of shock. However, it did not present new methodology or new mathematical formularization for solution of this problem.

The objective of this work is to analyze inner explosion in a corroded tube, with corrosion depth 50% and 75% of wall thickness using Autodyn software.

2. EMPIRICAL METHODS

There are several empirical methods proposed by researchers in order to calculate the peak pressure due to a blast wave produced by explosion in the air. These methods use experimental data to obtain polynomial equation, and depending on procedure and instrument employed by each author in the filed test, the equation can assume different forms and accuracy. As the blast wave propagate in a circular form, then these empirical equations use the distance (R, in m) between the detonation point and the point of measurement as a principal parameter, as well as, the quantity of explosive (Q, in kg). Some well known empirical method will be presented below.

The empirical formulae for peak pressure in air atmosphere proposed by Brode's consider different equations for different magnitude of peak pressure, as showed by equation (1) and (2) below. In this case, the pressure as result should be estimated *a priori*.

$$P_{so} = 0.67 \left(\frac{R}{Q^{1/3}} \right)^{-3} + 0.1, \quad P > 1 \text{ (MPa)} \quad (1)$$

$$P_{so} = 0.098 \left(\frac{R}{Q^{1/3}} \right)^{-1} + 0.1465 \left(\frac{R}{Q^{1/3}} \right)^{-2} + 0.585 \left(\frac{R}{Q^{1/3}} \right)^{-3} - 0.0019, \quad (2)$$

$$0.01 \leq P \leq 1 \text{ (MPa)}$$

Another method proposed by Henrych has considered the blast wave propagates in an unlimited atmosphere. The Henrych empirical formulae consider the ratio of distance and explosive mass as a principal parameter of variation. The evaluation of peak pressure can be made in the function of distance and explosive. These equations (3) – (5) are presented below.

$$P_{so} = 1.4072 \left(\frac{R}{Q^{1/3}} \right)^{-1} + 0.554 \left(\frac{R}{Q^{1/3}} \right)^{-2} - 0.0357 \left(\frac{R}{Q^{1/3}} \right)^{-3} + 0.0000625 \left(\frac{R}{Q^{1/3}} \right)^{-4}, \quad (3)$$

$$0.1 \leq R/Q^{1/3} \leq 0.3$$

$$P_{so} = 0.619 \left(\frac{R}{Q^{1/3}} \right)^{-1} - 0.033 \left(\frac{R}{Q^{1/3}} \right)^{-2} + 0.213 \left(\frac{R}{Q^{1/3}} \right)^{-3}, \quad 0.3 \leq R/Q^{1/3} \leq 1 \quad (4)$$

$$P_{so} = 0.066 \left(\frac{R}{Q^{1/3}} \right)^{-1} + 0.405 \left(\frac{R}{Q^{1/3}} \right)^{-2} + 0.329 \left(\frac{R}{Q^{1/3}} \right)^{-3}, \quad 1 \leq R/Q^{1/3} \leq 10 \quad (5)$$

Chengqing et. al. (2005) carried out a study making the comparison between experimental data and empirical method presented above. Based on the result of comparison, the authors made another proposal to estimate the peak pressure with higher accuracy. Such equations is been showed below.

$$P_{so} = 1.059 \left(\frac{R}{Q^{1/3}} \right)^{-2.56} - 0.051, \quad 0.1 \leq R/Q^{1/3} \leq 1 \quad (6)$$

$$P_{so} = 1.008 \left(\frac{R}{Q^{1/3}} \right)^{-2.01}, \quad 1 \leq R/Q^{1/3} \leq 10 \quad (7)$$

Chengqing et. al. (2005) also made the analysis to obtain the equation for propagation time evaluation. And made a relation between the empirical equation defined uniquely by explosive mass and distance, and the time, which is a important parameter as well, due to the dynamic natural of phenomenon.

All empirical equations presented above, doesn't consider the solid – fluid interaction, which is one of most important physical phenomenon is the blast wave propagation. Once the explosion occurs, it will produce a successive front of shock, which will attain the tube and return. When the first front of shock returns and the second front of shock advance, it will produce turbulence in the flow. Such interaction requires a complex numerical analysis, which wasn't

taken in account by the above empirical method. Due to this reason, the present work will employ numerical method, by using commercial software, AUTODYN.

3. NUMERICAL METHODS

To analyze problems of fluid structure interaction, two different approaches are commonly used: Eulerian formulation and Lagrangian Formulation. The Lagrange formulation adopt numerical mesh that moves and distorts with the material motion. The advantage of such a scheme is that the motion of material is tracked very accurately. Material interfaces and free surfaces are clearly defined. Also, history dependent material behavior is readily treated. The primary disadvantage of the Lagrange formulation is that for severe material deformations or flow, the numerical mesh will also become highly distorted with attendant loss of accuracy and efficiency or outright failure of the calculation. Typically, a Lagrange formulation is best suited for structural materials but not fluids or gases.

As mentioned above, Lagrange solvers are one of the basic models used in hydrocodes. One of the distinguishing features of a Lagrange code is that the grid it uses is created so that cell boundaries occur at free surfaces and material boundaries. Another is that during calculations, the mesh will distort to match the distortion of the material. In a typical Lagrange mesh, coordinates, velocities, forces, and masses are associated with the corner nodes, while stresses, strains, pressures, energies and densities are centered within the cells.

The main problems with Lagrange solvers occur when large deformations are involved. Severe distortion of the mesh can result in inaccuracies, negative densities and extremely small time steps. In order to avoid this situation, it may be necessary to eliminate the overly deformed cells by manually redrawing the mesh. Therefore, they are typically not used for models which involve flow or large distortion.

In the Euler formulation, the numerical mesh is fixed in space and material flows through it. The advantage of such a scheme is that large material flows and distortions can easily be treated. The disadvantage of such a scheme is that material interfaces and free surfaces are not naturally calculated. Sophisticated techniques must be utilized to track material interfaces. Additionally, history dependent material behavior is more difficult to track. In general, the Euler formulation is also more computationally intensive than Lagrange. Typically, the Euler formulation is best suited for fluid and gas behavior.

Instead of confining the grid to only the objects being modeled, Euler solvers place a grid over the space in which the materials can move. As the calculation progresses, the material of interest will move while the grid remains stationary. Individual nodes and cells are basically observing as the material being modeled flows by. In a typical Euler model, the centers of the cells are used as interpolation points for all variables, unlike Lagrange models as described above.

The main problems with Euler codes are with the amount of elements they require, and their poor handling of geometry. Since you are not only modeling the object of interest, but the space around that object, more elements and therefore more memory and time can be required than a standard Lagrange model. Also since the grid does not distort with the object of interest, it becomes more difficult to track the various components of a part, and therefore observe how a single piece behaves over time. Therefore, Euler models are typically not used to model solid objects.

The advantage of Euler solvers is that the mesh does not deform and therefore are not subject to the limitations imposed by deformations in Lagrange solvers. They can also allow the mixing of different materials inside the cells. Therefore, the shape of material surfaces is not completely limited by element size. They are used when a problem involves high levels of deformation or fluid flow, while Lagrange solvers are normally used to model solids which doesn't experience severe deformation.

4. APPLICATION

The air in the present work will use ideal gas as Equation of State (EOS). The explosive using TNT of 1g, and will adopt the equation of state JWL (Jones-Wilkens -Lee) as showing Equation (8).

$$P = C_1 \left(1 - \frac{\omega}{R_1 v} \right) \exp(-r_1 v) + C_2 \left(1 - \frac{\omega}{R_2 v} \right) \exp(-r_2 v) + \frac{\omega e}{v} \quad (8)$$

where v is the specific volume, e is specific energy. The values of constants C_1 , R_1 , C_2 , R_2 , ω for many common explosives have determined from dynamic experiments.

The following equation of state is used for air:

$$P = (\gamma - 1) \frac{\rho}{\rho_0} E \quad (9)$$

The tube has 50 mm diameter, with 1.5 mm as wall thickness. The material is assumed to present bilinear hardening behavior in order to simplify the phenomenon, with young's modulus 205 GPa, tangent modulus 75 GPa and 420 MPa as yield stress. With bilinear hardening material, it will be easier to validate fluid structure interaction, since the plastic effective strain will occur only after elastic regime, and will present linear behavior. A simplified 2D model was assumed to analyze the explosion in the tube, in order to reduce processing time and reduce computational effort. The analysis was carried out considering an Eulerian mesh for both air and TNT explosive. The air mesh has a dimension 100x100 mm with a unused area in the center. The unused area was filled with TNT material, with dimension 8x8 mm. Both air and TNT mesh have Euler element of 2x2 mm. The tube was model by Lagrangian elements, with 4 elements in the radial direction and 144 elements in circumferential direction. Such element is a quadrilateral element with 4 nodes. Two cases are studied in the present work, the first one is the tube with 50% of corrosion depth and the second case is 75%, as show the Figures 1 and 2.

There are seven points of measurement defined as gauges fixed in the space for pressure measurement. These points are suitable to capture solid – flow interaction, as well as, tube hardening behavior. The gauge 1 is located at the center of mesh, at the point of detonation ($x=50\text{mm}$, $y=50\text{mm}$). The gauge 2 was located at a point nearby the tube, in order to capture solid – fluid interaction ($x=30\text{ mm}$, $y=50\text{mm}$). The gauge 3 was located outside the tube ($x=20\text{mm}$, $y=50\text{mm}$), with the purpose to capture pressure variation during the explosion and solid expansion. The gauge 4 was located between gauge 1 and gauge 2 ($x=40\text{mm}$, $y=50\text{mm}$). The gauge 5 was fixed in the space and nearby to tube inner surface ($x=25\text{mm}$, $y=50\text{mm}$). There are two moving gauges defined in tube. The gauge 6 is a moving gauge in the inner surface of tube, following the tube expansion. The gauge 7 was defined on the corrosion region, outside the tube. The result of both cases will be presented in the following section.

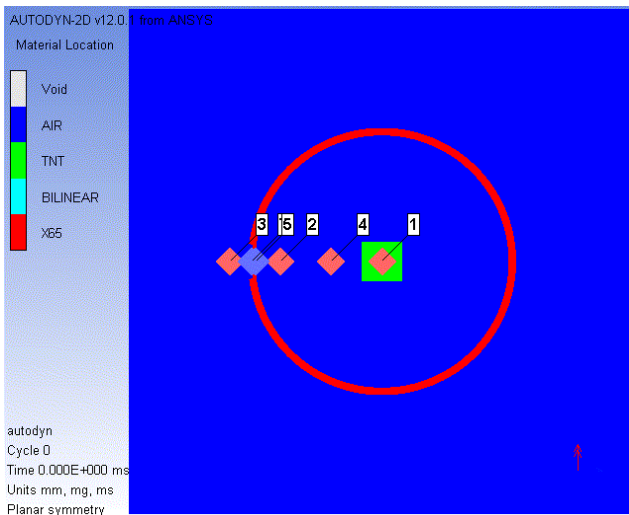


Figure 1 (a). 50% corrosion and position of gauges

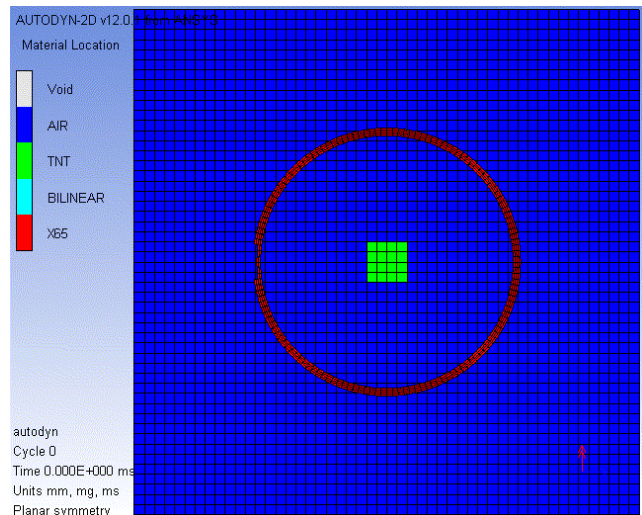


Figure 1 (b). Mesh of tube with 50% of corrosion.

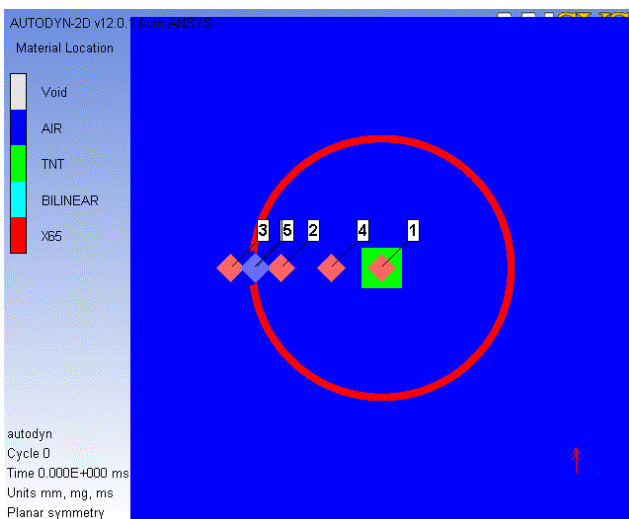


Figure 2 (a). 75% corrosion and position of gauges

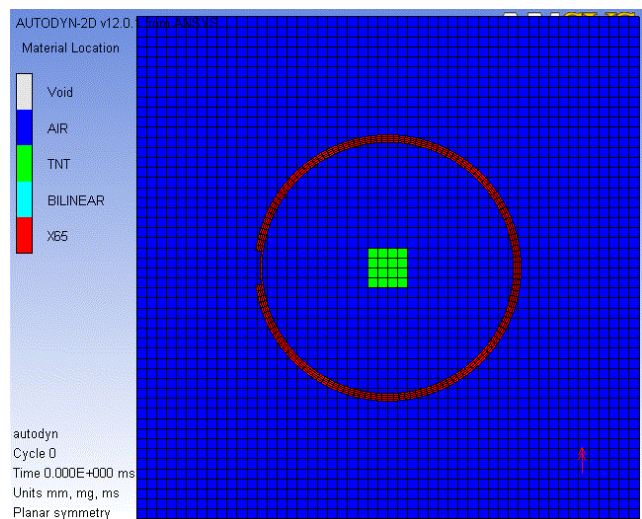


Figure 2 (b). Mesh of tube with 75% of corrosion.

5. RESULTS

The first case analyzed is the tube with 50% of wall thickness with corrosion. The solution procedure is interrupted after 12100 cycles due to numerical errors. It is possible to observe the stress concentration in the corrosion region, and at the vicinity of corners. The Figures 3 and 4 show the stress distribution at the tube.

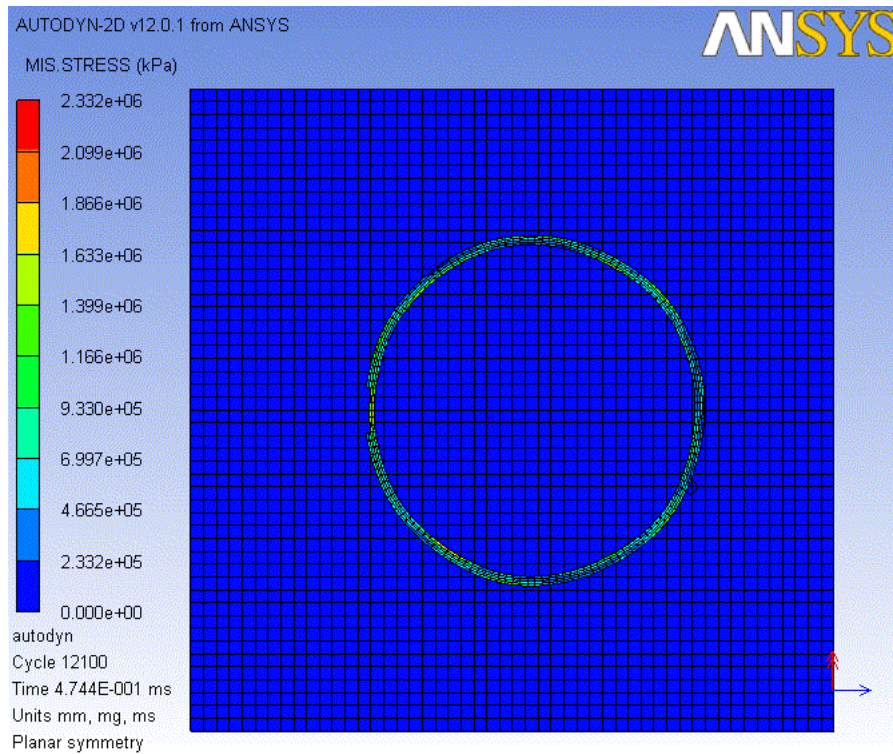


Figure 3. Distribution of stress in the tube with 50% of wall thickness as corrosion depth.

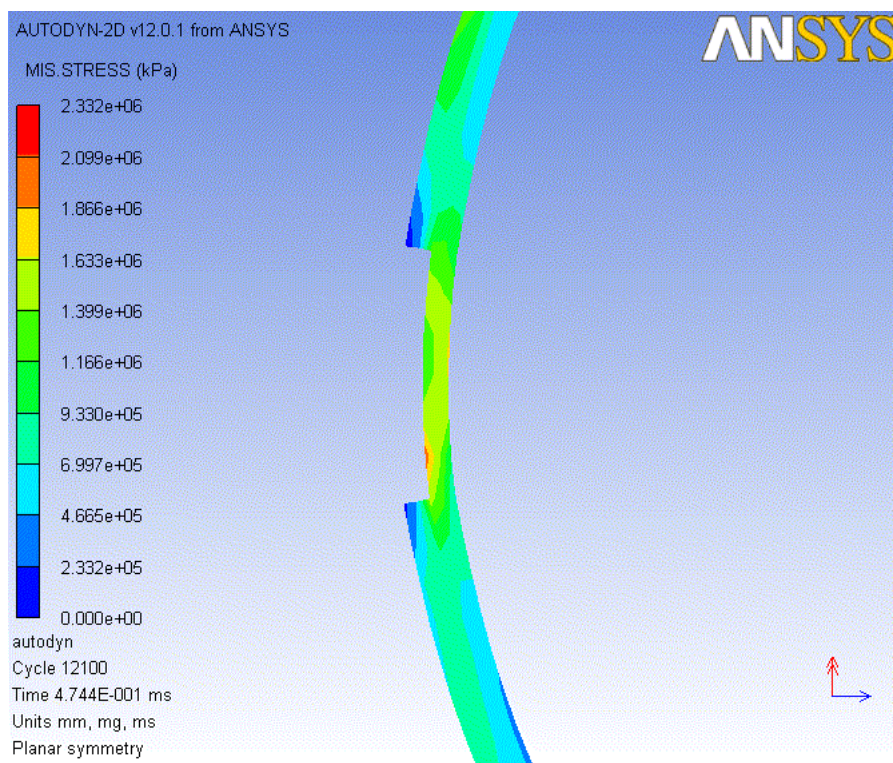


Figure 4. Zoom of the stress distribution at the region of corrosion of tube with 50% of wall thickness as corrosion depth.

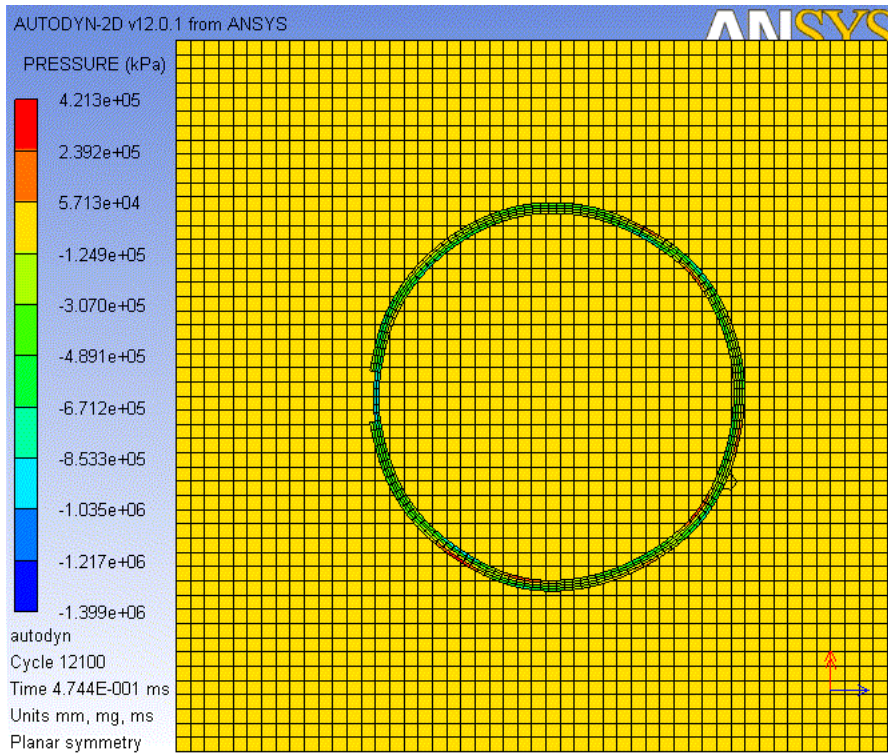


Figure 5. Pressure caused by detonation process at the cycle 12100.

The figure 5 shows the pressure in whole Eulerian and Lagrangian domain at the cycle 12100. According to solid – fluid interaction, the pressure acting on inner surface of tube suffers variation between a range, which can be observed in the figure 6(d). The pressure measured by gauge 6 shows an oscillation, probably produced by solid – fluid interaction, and especially by material hardening, which plays an important role in the interaction process. The figure 6(a) shows the pressure curve in the gauge 1, situated on detonation point. At the very beginning of detonation, the pressure produced near the point increase suddenly, then propagates in a circular form. The figure 6 (b) shows the pressure for gauge 2-5. It is possible to observe the visible pressure oscillation due to solid – fluid interaction. The gauge 5 doesn't register a visible oscillation after 0.1 ms.

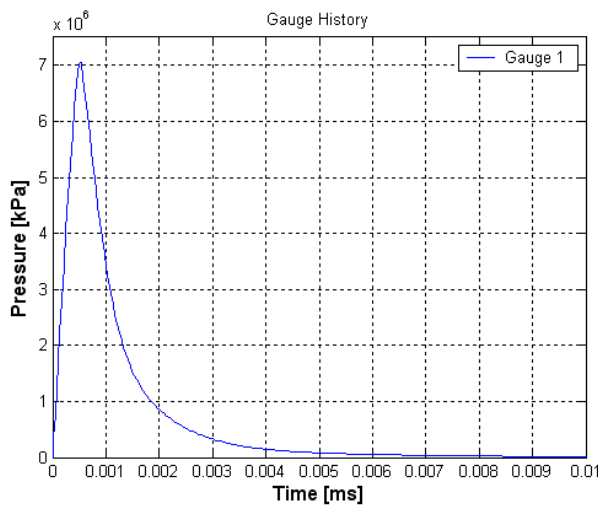


Figure 6 (a). Pressure of gauge 1.

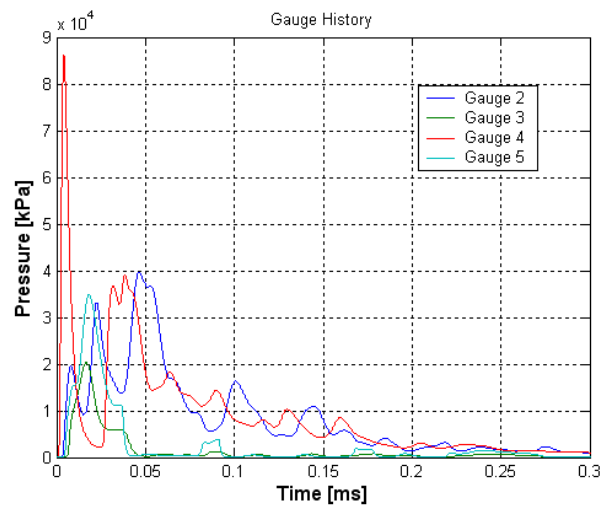


Figure 6 (b). Pressure of gauge 2-5.

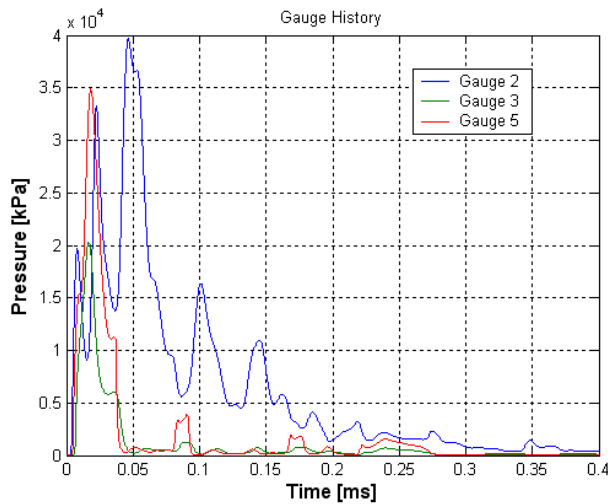


Figure 6 (c). Pressure of gauge 2, 3 and 5.

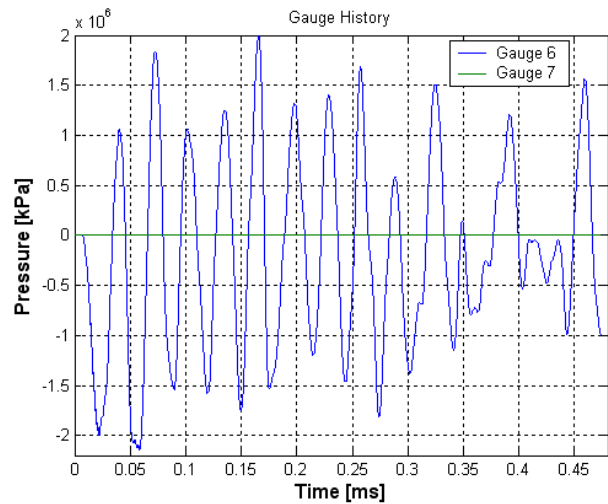


Figure 6 (d). Pressure of gauge 6 and 7.

In the figure 6(c) it is easier to observe the pressure oscillation at the gauge 2 and 5. The figure 6(d) shows a significant pressure oscillation at the point in the inner surface of tube, representing the oscillation pressure acting the tube, especially nearby the corrosion region. The oscillation captured by gauge 6 could be a result of solid-fluid interaction, also the material bilinear hardening. While the blast wave acts on the surface, the tube expands and deforms according to material hardening equation, and the fluid blast wave returns. All these reasons produced the visible oscillation in figure 6(d).

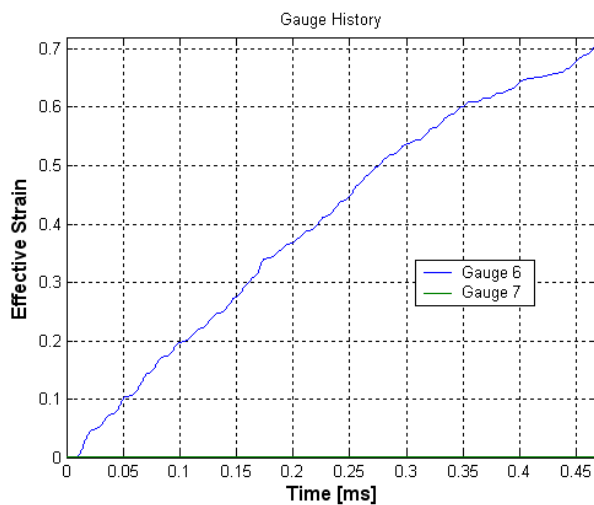


Figure 7 (a). Effective strain captured by gauge 6 and 7 in the case of 50% corrosion depth.

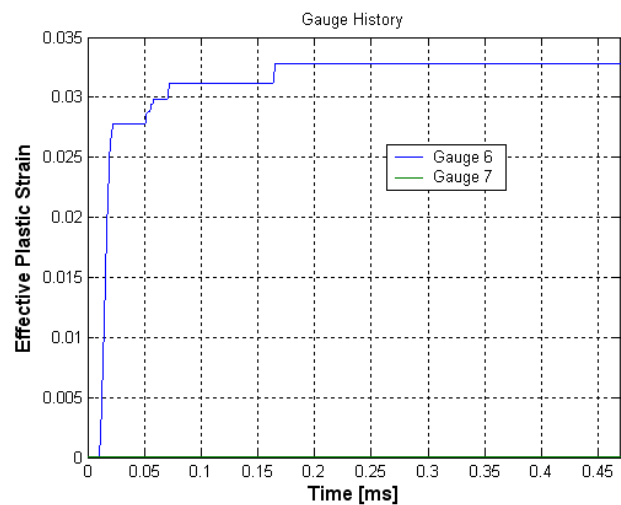


Figure 7(b). Effective plastic strain in the inner surface, near to corrosion region.

Figures 7 (a) - (b) show the strain captured by gauge 6 and 7. Figure 7 (a) show the effective strain measured by gauge 6, which varies almost linearly. At the same time, the gauge 7 doesn't capture any significant variation at the outside surface of tube. Figure 7(b) shows the effective plastic strain of gauge 6. As the material of tube is bilinear hardening, therefore it is reasonable for the figure to show a significant variation from time 0.03 ms to 0.17 ms. During this period of time, the solid - fluid interaction produce a pressure oscillation and cause a deformation, at the same time as the material suffer a hardening, according to Von Mises equation government.

In the case below, the 75% wall thickness of corrosion depth is analyzed. In the figure 8(a)-(b), the distribution of pressure at cycle 15910 is showed. Figure 8(a) shows the mesh of Eulerian elements and Figure 8(b) the Lagrange elements at this instance. The tube presents a deformation and ovalization, especially in the corrosion region. Such as showed by figure 9(a)-(b). The figure 9(b) shows a zoom in the corrosion region, and it is possible to observe a significant deformation in the corrosion area. As the pressure varies according to solid - fluid interaction, so the pressure inside the tube could have negative value, below the atmospheric pressure. This can be the reason for tube in cycle 15910 to present such a deformation profile.

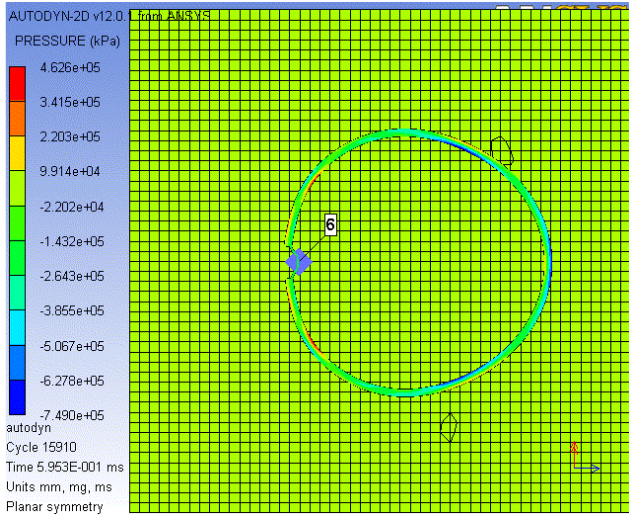


Figure 8(a). Pressure distribution at cycle 15910.

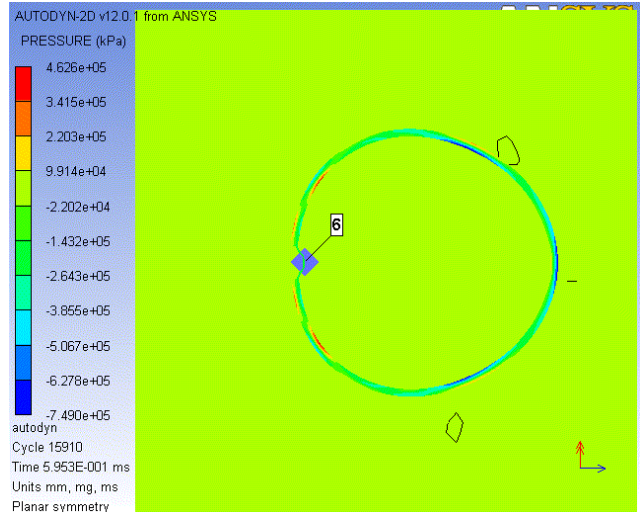


Figure 8 (b). Pressure distribution at cycle 15910.

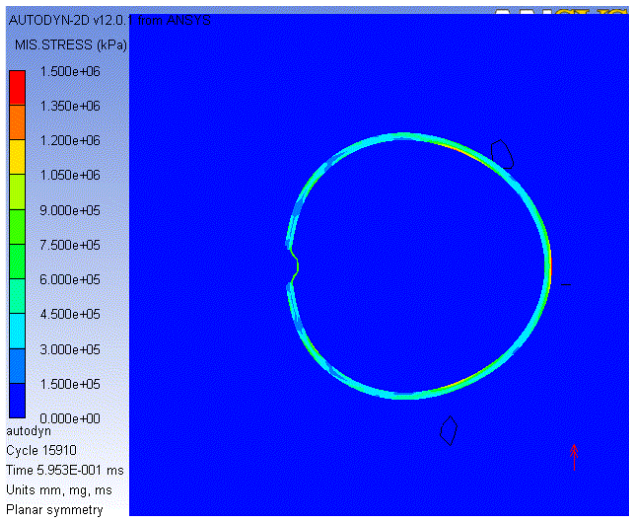


Figure 9 (a). Distribution of stress at cycle 15910 in the tube with 75% of thickness in corrosion depth.

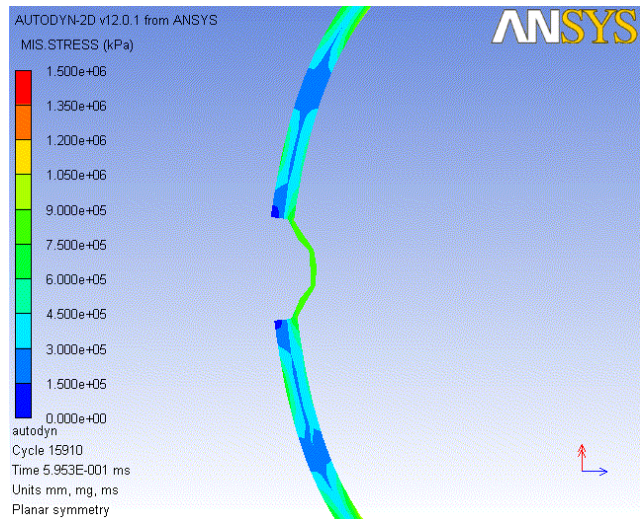


Figure 9 (a). Distribution of stress at cycle 15910 in the tube with 75% of thickness in corrosion depth, in the corrosion region.

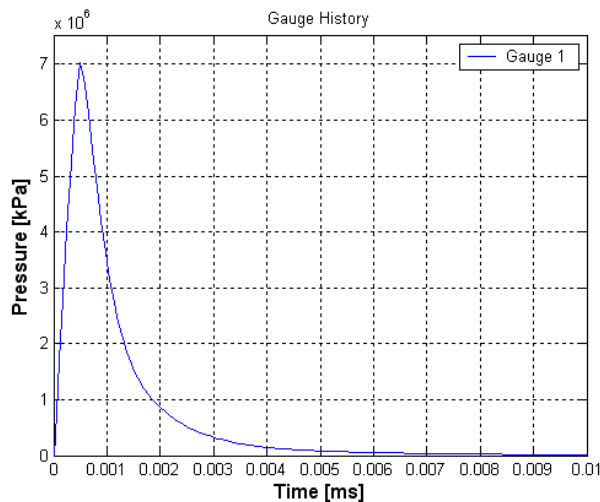


Figure 10 (a). Pressure captured by gauge 1, in case of 75% of corrosion depth.

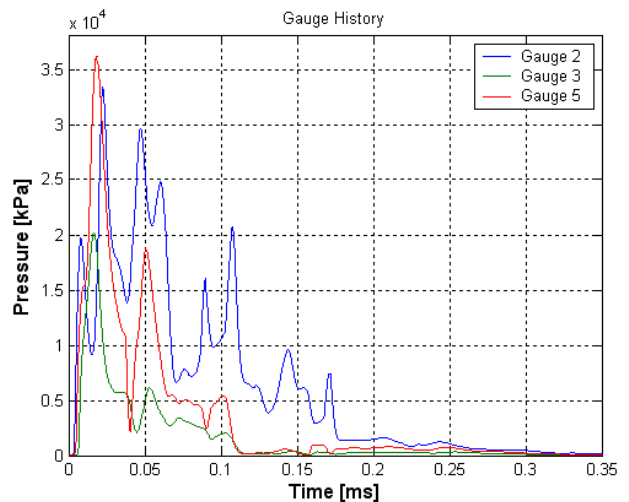


Figure 10 (b). Pressure captured by gauge 2, 3 and 5, in case of 75% of corrosion depth.

The figure 10(a) shows the pressure profile in the location of gauge 1. As it can be observed, the profile is exactly the same as the case of 50%. The figure 10(b) shows the pressure profile captured by gauge 2, 3 and 5. The profile oscillation is more intense in comparison to the case of 50% of corrosion depth. The reason could be higher deformation in the corrosion region, and consequently, the tube initiate the material hardening more rapidly. All this phenomenon contribute to the solid – fluid intense interaction and produce a pressure profile with more significant oscillation. Nevertheless, the oscillation tends to a stationary state after 0.2 ms. After this instance, the pressure profile captured by gauge 6 also presents the same behavior, showed by figure 10 (d), as well as the gauge 4, in the Figure 10 (c). All this information indicate that the tube with lower remaining strength (25% remaining strength) is more sensitive to solid – fluid interaction and initiate material hardening at lower pressure. But after a period of time, it tends to a stationary state, different to the case of 50% of corrosion depth, which presents pressure oscillation more regular and time depending.

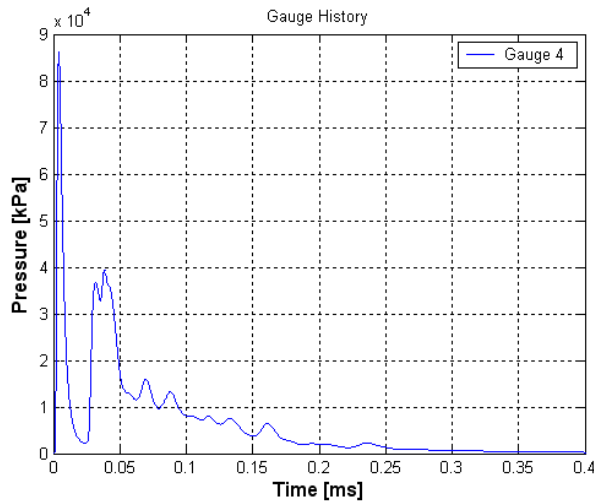


Figure 10 (c). Pressure captured by gauge 4, in case of 75% of corrosion depth.

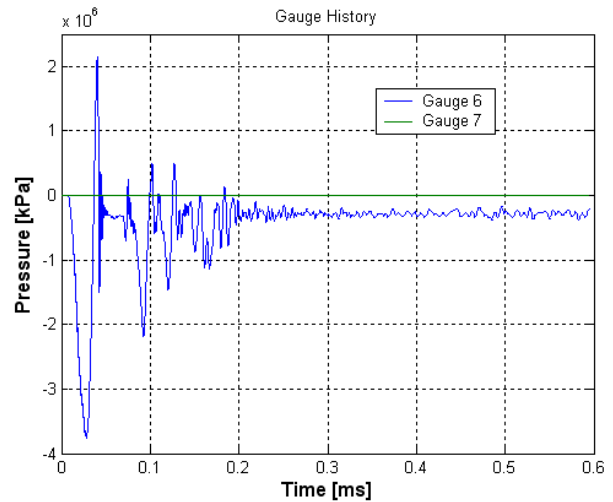


Figure 10 (d). Pressure captured by gauge 6 and 7, in case of 75% of corrosion depth.

The figure 11(a)-(b) show the strain at the inner surface and outer surface of tube. As it can be observed, the strain at the inner surface varies according to pressure oscillation, but after 0.2 ms, the strain tends to a value. By the other hand, the figure 11 (b) indicates the material hardening at the early stage of analyze.

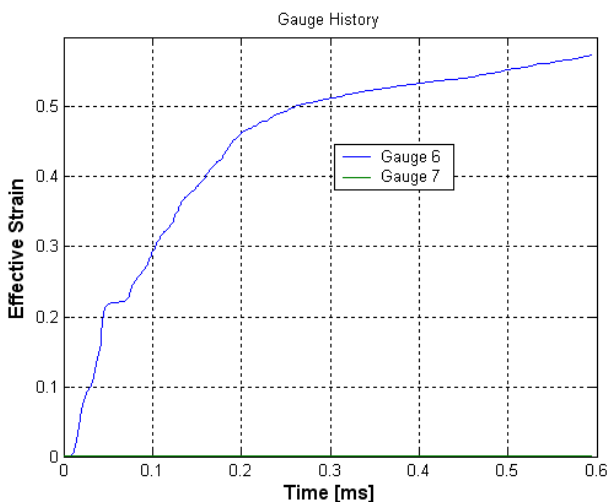


Figure 11(a). Effective strain in gauge 6 and gauge 7, in the case of 75% of corrosion depth.

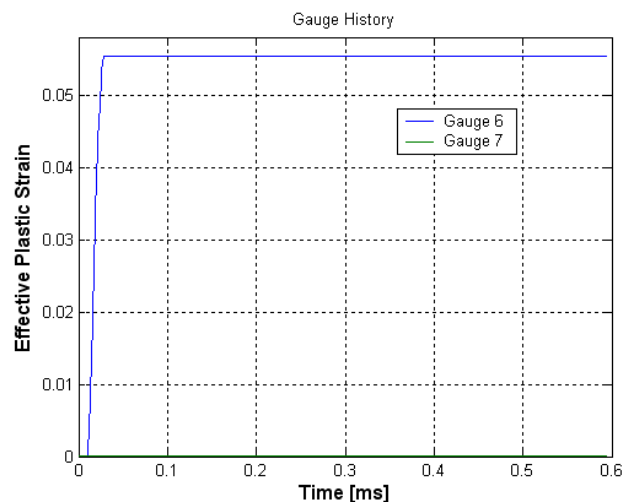


Figure 11(b). Effective plastic strain in gauge 6 and gauge 7, in the case of 75% of corrosion depth.

6. CONCLUSION

From the results obtained in the above 2 cases, it is possible to observe the tube with deeper corrosion is more sensitive to explosion and answer in higher magnitude in pressure wave, produced by solid – fluid interaction. After a period of time, the pressure and wall deformation tend to a stationary behavior and converge to a value. The energy released by explosion was absorbed by tube deformation, and the tube performed hardening behavior to absorb this

energy. In the case of tube with 50% corrosion depth, the tube seen to interact in a period of time longer than 75% of corrosion depth. The energy released by explosion was also absorbed by hardening behavior. However, as the wall thickness has more material, than it is possible for a part of material to absorb the energy and initiate plastic hardening, while the residual part remains elastic and interact with fluid producing pressure oscillation

7. REFERENCES

Autodyn – ANSYS INC.

Chan, C. Y. & Kong, P. C. 1995, “A thermal explosion model”, *Applied Mathematics and Computaciona*, Vol.71, pp.201-210.

Chengqing Wu, Hong Hao, 2005, “Modeling of simultaneous ground shock and airblast pressure on nearby structures from surface explosions”. *Int. J. Impact Eng*, Vol. 31, pp. 699-717

Kwon, Y. W. & Cunningham, R. E., 1998, “Comparison of Usa-Dyna finite element models for a stiffened shell subject to underwater”, *Computer & Structure*, Vol.66, No.1, pp127-144.

Lu, y. & Wang, Z., 2006, “Characterization of structural effects from above-ground explosion using coupled numerical simulation”, *computer & Structure*, Vol.84, pp. 1729-1742.

Ritsu Dobashi ,1996, “Experimental study on gas explosion behavior in enclosure”, *J. Loss Prev. Process Ind*, Vol.10, No2. pp. 83-89.

Wu, C. & Hao, H., 2005, “Modeling of simultaneous ground shock and airblast pressure on nearby structures from surface explosions”, *International Journal of Impact Engineering*, Vol. 31, pp. 699-717.

Zyskowski, A., Sochet, I., Mavrot, G., Bailly, P. & Renard J. 2004, “Study of the explosion process in a small scale experiment – structural loading”, *J. Loss Prev. Process Ind*, vol. 17, pp. 291-299.

8. RESPONSIBILITY NOTICE

The authors are the only responsible for the printed material included in this paper.